Noncontact Steering of Magnetic Objects by Optimal Linear Feedback Control of Permanent Magnet Manipulators

Nayereh Riahi and Arash Komaee

***Abstract*— A magnetic manipulator for noncontact steering of magnetic objects is considered. This system utilizes a flexible array of permanent magnets, each equipped with a servomotor to independently control its direction. The total magnetic field produced by the magnets can be shaped effectively by adjusting the directions of all magnets, which in turn, provides an effective control over the magnetic force it applies to a magnetic object. The dynamics of this object under such controlled magnetic force is inherently unstable and is represented by a set of highly nonlinear state-space equations. Despite the nonlinear nature of these equations, it is shown that an optimally designed linear state feedback can successfully stabilize the object and steer it along arbitrary reference trajectories inside a reasonably large operation region. The key to this success is the optimal scheme of this paper for linearizing the dynamics of the magnetic object.**

I. Introduction

This paper is a follow up to our previous work on design, optimization, and feedback control of noncontact permanent magnet manipulators [1], [2]. Magnetic manipulators consist of arrays of magnets (electromagnet or permanent magnet) to generate and precisely control magnetic fields, which interact with magnetic objects or fluids inside their operation region to control them from a distance without a direct mechanical contact [1]–[10]. Application of feedback control enables the magnetic manipulators to drive magnetic objects precisely in the directions required to perform certain tasks, for instance, tracking a reference trajectory at a desired speed [1], [7], [8].

Since magnetic fields can propagate through nonmagnetic barriers, they provide a unique ability to manipulate magnetic objects behind such physical barriers without a direct contact. This *noncontact* feature is successfully exploited in magnetic manipulators for safe and precise operation of magnetically driven medical tools inside the human body for noninvasive surgical, imaging, and drug targeting procedures [11]–[21]. Furthermore, this feature is essential for actuating micro- and nanoscale systems in which a direct contact for manipulation and control is not feasible [22]–[27].

Our work principally focuses on permanent magnets as the source of magnetic field, in opposition to the dominant trend in most prior work that relies on electromagnets. The major advantage of electromagnets over permanent magnets is their easy control of magnetic field simply through their terminal voltages. Hence, a spatially fixed array of electromagnets can generate a controllable magnetic field simply by adjusting the relative strength of their fields through their voltages [3]–[9]. Despite this key advantage, the downside of electromagnets is their weak magnetic fields compared to their size, weight, cost, and power consumption. For most medical applications, which typically need strong magnetic forces at relatively long distances (several decimeters), the required electromagnets will be substantially large, heavy, and expensive. In addition, large electromagnets consume large amounts of energy, need cooling systems, and demonstrate slow dynamics (large time constant) that turns them difficult to control.

On the other hand, permanent magnets offer a much higher strength-to-size ratio compared to electromagnets: 1 cm^3 of a rare-earth magnet can produce magnetic fields equivalent to an electromagnet with some kilowatts power [10]. Besides, permanent magnets do not require external sources of power to operate, which renders them an attractive choice to design compact, effective, and inexpensive magnetic manipulators. The magnetic field in a permanent magnet manipulator must be controlled mechanically by altering the spatial position of its magnets, which indeed requires more complex design and implementation to integrate mechanical actuators as means of control. Even with this added complexity, permanent magnets present a practical alternative (if not the only alternative) to electromagnets in those applications that need large magnetic forces at distances of some decimeters.

This paper considers a magnetic manipulator consisting of permanent magnets and mechanical actuators, schematically shown in Fig. 1. We first introduced this manipulator in [1] and further studied its feedback control in [2]. The proposed setup is designed to control the planar motion of a magnetic bead inside a circular flat container filled with a viscous fluid. An array of $n = 6$ radially magnetized permanent magnet discs is arranged around the container at equal distances. Each magnet is equipped with a servomotor to freely control its angular position, and thereby, the direction of its magnetic field. The servomotors are internally equipped with feedback loops, which enable them to rapidly change the direction of the magnets, as required. The total magnetic field inside the circular container is controlled by adjusting the directions of all n magnets, which in turn, provides an effective control over the magnetic force applied to the magnetic bead in the plane of motion.

The precise directions of all $n = 6$ magnets is determined by a feedback controller in terms of the position and velocity vectors of the magnetic bead. To establish a feedback control, these vectors are directly measured by a sensing device. In an experimental setup we are currently prototyping, this sensing device is an optical camera equipped with image processing

This work was supported by the National Science Foundation under Grant ECCS-1941944.

The authors are with the Department of Electrical and Computer Engineering, Southern Illinois University, Carbondale, IL, 62901 USA email: {nayereh.riahi, akomaee}@siu.edu.

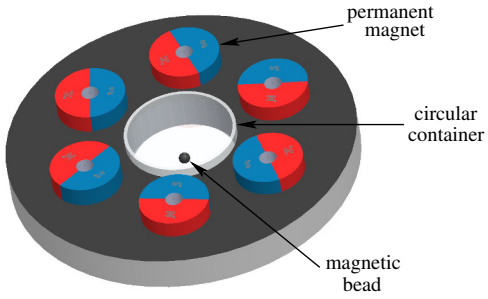

Fig. 1. Schematic diagram of a magnetic manipulator with $n = 6$ radially magnetized permanent magnet discs equally spaced around a circular flat container.

and estimation techniques for tracking the magnetic bead. In medical applications, the sensing device can be a real-time medical imaging system based on fluoroscopy [28].

Feedback control is an essential component of all magnetic manipulators utilized for motion control of magnetic objects. Application of feedback for motion control is required by the very nature of magnetic fields. By Earnshaw's theorem [29], magnetic fields are unstable in the sense that the trajectories of multiple magnetic particles moving under magnetic force are divergent, even if they start at a very close distance [21]. Hence, any effort to control the motion of magnetic objects in a magnetic field will eventually lead to some sort of feedback stabilization problem.

The focus of this paper is on design of a feedback control law that enables the magnetic manipulator of Fig. 1 to drive the magnetic bead along an arbitrary reference trajectory. A major challenge in development of such feedback law is the highly nonlinear dynamics of this magnetic manipulator. In our prior work, we proposed a feedback linearization scheme to effectively compensate for the nonlinearity of the magnetic manipulator [1], [2]. To implement such exact linearization, an inverse problem is solved in real time, seeking the angular position of all magnets to generate a required magnetic force at the current location of the magnetic bead. This inverse problem is defined by a system of highly nonlinear algebraic equations with excessive computational complexity for real-time implementation. Furthermore, this system of equations involves some analytical model for the magnetic field of each magnet, which is difficult to obtain and typically imprecise.

The goal in this paper is to develop a practical control law with an affordable computational complexity, and with a few parameters that can be easily tuned by direct measurement of the magnetic field at a few spatial points inside the operation region of the magnetic manipulator. Unlike the more complex nonlinear control we developed in [1], [2], this simple control law is not expected to perform uniformly well over the entire operation region of the magnetic manipulator. Alternatively, it is optimized for a reasonable performance over the largest possible subregion, which can be sufficient for some, but not all, applications. We are currently working to expand this subregion by means of gain scheduling [30]. The core idea is to design multiple control laws for several overlapping subregions, and smoothly switch between them as the magnetic object moves from one subregion to another.

The control design approach adopted in this paper relies on approximate linearization of the magnetic manipulator, and then using a standard method of linear state feedback design such as the method of linear quadratic regulator (LQR) [31]. This simple approach is then enhanced by a novel technique to optimize the operating point at which the dynamics of the magnetic manipulator is linearized. Our simulation results indicate that this technique drastically improves the control performance in terms of stability and the size of region over which the magnetic bead can be precisely steered.

The linear control law in this paper exhibits a new feature not adequately addressed in our prior work. In this paper, the intrinsic low-pass dynamics of the servomotors is properly involved in the dynamical model of the magnetic manipulator and in the control design procedure. This low-pass dynamics potentially has a notable effect in the overall performance of the magnetic manipulator, which was simply neglected in our previous work [1], [2].

II. Dynamical Model

This section presents a mathematical model to describe the motion of a magnetic bead inside the circular container of the magnetic manipulator in Fig. 1. This model is a more realistic version of the one introduced in [1], in the sense that the new model includes the low-pass nature of the servomotors. In developing this model, two planar coordinate systems shown in Fig. 2 are utilized. The reference coordinate system in Fig. 2(a) is fixed with respect to the magnetic manipulator and its origin is at the center of the circular container. In this coordinate system, the position of the magnetic bead is represented by $r = [r_1 \quad r_2]^T$ and the set of points inside the circular container of radius a is denoted by $\mathscr{C} \subset \mathbb{R}^2$.

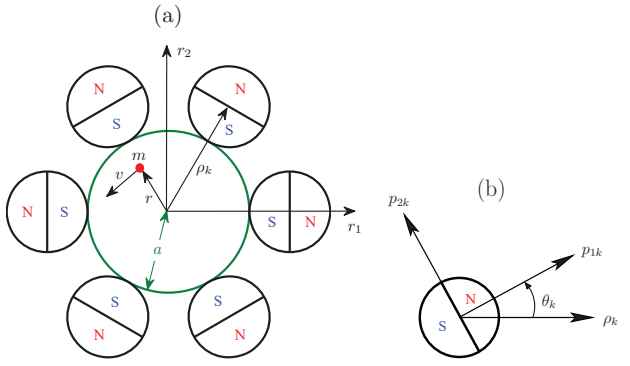

Fig. 2. Planar diagram of the magnetic manipulator of Fig. 1 along with (a) reference coordinate system, and (b) local coordinate system for magnet k with the rotation angle θ_k.

The magnetic bead is manipulated by n identical radially magnetized permanent magnet discs of radius b. The magnets are equally spaced around the circular container at a distance $a+b$ from its center. In the reference coordinate system, the center of the kth magnet is fixed at the point

$$\rho_k = (a+b)\,[\cos\phi_k \quad \sin\phi_k]^T, \quad \phi_k = \frac{2\pi\,(k-1)}{n}.$$

The direction of this magnet is characterized by an angle θ_k measured counterclockwise between vector ρ_k and its north

pole. A local coordinate system shown in Fig. 2(b) is fixed to each magnet with the origin at the center of the magnet and the first orthogonal axis aligned with its north pole.

Consider a point in the circular container and represent it in the reference coordinate system by r. The representation of this point in the local coordinate system attached to magnet k is denoted by p_k and is determined by a linear transformation of r that consists of a translation by ρ_k followed by a rotation of angle $\theta_k + \phi_k$. This linear transformation is given by

$$p_k = R^T(\theta_k + \phi_k)(r - \rho_k), \tag{1}$$

where $R(\varphi) = [\cos\varphi, -\sin\varphi; \sin\varphi, \cos\varphi]$ is a 2×2 rotation matrix.

Suppose the vector function $h_c(\cdot) : \mathbb{R}^2 \to \mathbb{R}^2$ represents the magnetic field of each magnet in its own local coordinate system. Then, the magnetic field of magnet k is represented in the reference coordinate system via the rotation of $h_c(p_k)$ by the angle $-(\theta_k + \phi_k)$, i.e., $R(\theta_k + \phi_k) h_c(p_k)$. By (1), the contribution of magnet k at a point $r \in \mathscr{C}$ is expressed in the reference coordinate system by

$$h_k(r, \theta_k) = R(\theta_k + \phi_k) h_c\left(R^T(\theta_k + \phi_k)(r - \rho_k)\right).$$

The total magnetic field $h(r, \theta)$ produced by n magnets at a point $r \in \mathscr{C}$ is the superposition of the contributions of all n magnets, that is

$$h(r, \theta) = \sum_{k=1}^{n} R(\theta_k + \phi_k) h_c\left(R^T(\theta_k + \phi_k)(r - \rho_k)\right).$$

Here, $\theta = [\theta_1 \quad \theta_2 \quad \cdots \quad \theta_n]^T$ is an $n \times 1$ vector containing the rotation angles of all n magnets.

The total magnetic force applied to a magnetic bead at a point $r \in \mathscr{C}$ of the circular container is given by [32], [33]

$$f_{mag}(r, \theta) = k_m \nabla \|h(r, \theta)\|^2,$$

where k_m is a positive constant depending on the volume and permeability of the magnetic bead, ∇ is the gradient operator with respect to r, and $\|\cdot\|$ represents the Euclidean norm. This expression is rewritten in the more compact form

$$f_{mag}(r, \theta) = k_m g(r, \theta) \tag{2}$$

by defining the vector function $g(\cdot) : \mathbb{R}^2 \times \mathbb{R}^n \to \mathbb{R}^2$ as

$$g(r, \theta) = \nabla \|h(r, \theta)\|^2.$$

The magnetic bead moves inside a viscous fluid under the magnetic force (2) and the drag force f_{drag}. By Stokes' drag law, this latter force linearly depends on the velocity v of the magnetic bead [33], [34], that is

$$f_{drag} = -\mu v. \tag{3}$$

Here, μ is the friction coefficient, which is a positive constant depending on the diameter of the magnetic bead and the viscosity of its surrounding fluid [33], [34].

Newton's second law of motion is applied to the magnetic bead of mass m to obtain the differential equation

$$m\dot{v}(t) = f_{mag}(r(t), \theta(t)) + f_{drag}(t).$$

Substituting (2) and (3) into this equation, and then defining the positive constants $\sigma_v = \mu/m$ and $k_g = k_m/\mu$ lead to

$$\dot{v}(t) = \sigma_v k_g g(r(t), \theta(t)) - \sigma_v v(t). \tag{4}$$

The direction of each permanent magnet is independently controlled by a servomotor. The servomotor k is regarded as a dynamical system with a scalar input $u_k(t)$ and a scalar output $\theta_k(t)$. Each servomotor is described by a first order linear system with the time constant τ; hence, the dynamics of all n servomotors is represented in vector form by

$$\dot{\theta}(t) = -\sigma_s \theta(t) + \sigma_s u(t), \tag{5}$$

where $\sigma_s = 1/\tau$ is a constant and $u = [u_1 \quad u_2 \quad \cdots \quad u_n]^T$ is a control vector including n scalar inputs to the servomotors. This dynamics was neglected in our prior work for simplicity of controller design [1], [2].

To describe the overall dynamics of the magnetic bead, the state-space equations (4), (5), and $\dot{r} = v$ are gathered into

$$\dot{r}(t) = v(t) \tag{6a}$$

$$\dot{v}(t) = \sigma_v k_g g(r(t), \theta(t)) - \sigma_v v(t) \tag{6b}$$

$$\dot{\theta}(t) = -\sigma_s \theta(t) + \sigma_s u(t). \tag{6c}$$

These equations represent a nonlinear dynamical system with the state vector $x(t) = (r(t), v(t), \theta(t))$ in $\mathbb{R}^{n+4}$ and the control vector $u(t)$ in $\mathbb{R}^n$. This state vector is directly measured to establish a linear feedback control, as shown in Fig. 3. The purpose of this controller is to generate a control vector $u(t)$ such that the position $r(t)$ of the magnetic bead closely tracks a desired reference trajectory $r_d(t) \in \mathscr{C}$.

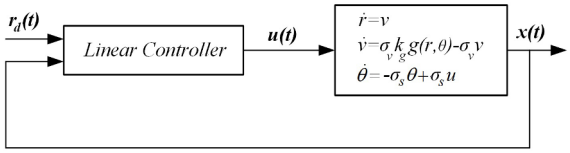

Fig. 3. Block diagram of closed-loop system with a linear controller.

III. Controller Design

The goal of this section is to develop an easy to implement linear controller for the magnetic manipulator of Fig. 1. Of course, the state-space equations (6) that describe this system are inherently nonlinear through the nonlinear function $g(\cdot)$. Hence, the simple approach adopted here is to linearize these equations around some equilibrium of the system, and then, design a linear control law for the approximate linear model. This procedure results in a family of linear control laws that depend on the equilibrium point at which the dynamics (6) is linearized. Then, this equilibrium point is optimized for the best closed-loop performance.

A. Linearized Model

Our focus is on steering magnetic objects near the center of the circular container in Fig. 1, therefore an equilibrium is chosen at $r = 0$. Let θ_e be any $n\times1$ constant vector satisfying

$$g(0, \theta_e) = 0. \tag{7}$$

Then, the constant control $u = \theta_e$ applied to the servomotors creates an equilibrium of (6) at $(r, v, \theta) = (0, 0, \theta_e)$. In order to linearize (6) around this equilibrium, the Taylor expansion of $g(\cdot)$ and (7) are used to approximate

$$g(r, \theta) \simeq G_r(0, \theta_e) r + G_\theta(0, \theta_e)(\theta - \theta_e),$$

where $G_r(\cdot)$ and $G_\theta(\cdot)$ are 2×2 and $2 \times n$ matrices denoting the Jacobian of $g(r, \theta)$ with respect to r and θ, respectively. Then, the linear approximation of (6) is expressed as

$$\dot{x}_e(t) = A x_e(t) + B u_e(t) \tag{8a}$$
$$r(t) = C x_e(t), \tag{8b}$$

where $x_e = (r, v, \theta - \theta_e)$ is the state vector, $u_e = u - \theta_e$ is the control vector, and matrices A, B, and C are defined as

$$A = \begin{bmatrix} 0_{2\times2} & I_{2\times2} & 0_{2\times n} \\ \sigma_v k_g G_r(0, \theta_e) & -\sigma_v I_{2\times2} & \sigma_v k_g G_\theta(0, \theta_e) \\ 0_{n\times2} & 0_{n\times2} & -\sigma_s I_{n\times n} \end{bmatrix} \tag{9}$$
$$B = \begin{bmatrix} 0_{2\times n} \\ 0_{2\times n} \\ \sigma_s I_{n\times n} \end{bmatrix}, \quad C = \begin{bmatrix} I_{2\times2} & 0_{2\times2} & 0_{2\times n} \end{bmatrix}.$$

Note that the approximate model (8) depends on the actual value of θ_e, which is optimized later in Section III-C to attain the best closed-loop performance.

In opposition to the nonlinear state-space equation (6) that requires the complete knowledge of the magnetic field $h_c(\cdot)$, the linearized model (8) only needs partial knowledge of the magnetic field to compute matrices $G_r(0, \theta_e)$ and $G_\theta(0, \theta_e)$. Instead of relying on the theoretical models of the magnetic field, these matrices can be estimated experimentally from measurements of the magnetic field recorded at certain points around $r = 0$. This helps to fill a possible gap between theory and practice when tuning the linear controller designed based on the approximate model (8).

It is worth mentioning that the linear system (8) is unstable in nature, i.e., matrix A has at least one positive eigenvalue. This essential property is independent of the point at which the original system is linearized, and is a result of Earnshaw's theorem [29] that implies the Jacobian matrix $G_r(r, \theta)$ of a magnetic force has at least one positive eigenvalue at every point r [16], [21].

B. State Feedback Control

Despite the fact that (8a) characterizes an unstable system, it can be stabilized using a state feedback law [31]. Consider a simple scenario under which the magnetic bead starts from an initial point $r \neq 0$ near the center of the container (see Fig. 1), and is steered toward the equilibrium at $r = 0$. This control goal can be achieved via the method of LQR [31] by minimizing the quadratic cost function

$$J = \int_0^\infty \left(x_e^T(t) Q x_e(t) + u_e^T(t) R u_e(t) \right) dt. \tag{10}$$

This cost function simultaneously penalizes deviations of the state vector $x_e(t)$ (i.e., position and velocity) and the control vector $u_e(t)$ from the desired value of 0. The positive semi-definite matrix Q and the positive definite matrix R adjust the relative importance of the deviations in state and control.

It is well-known [31] that this cost function is minimized by the stabilizing linear state feedback

$$u_e(t) = -K x_e(t), \tag{11}$$

where $K = R^{-1} B^T P$ is an $n \times (n + 4)$ gain matrix. Here, P is a positive definite matrix and the solution to the algebraic Riccati equation

$$A^T P + P A - P B R^{-1} B^T P + Q = 0. \tag{12}$$

The linear control law (11) is explicitly expressed in terms of the state and control of the original system (6) as

$$u(t) = -K_r r(t) - K_v v(t) - K_\theta(\theta(t) - \theta_e) + \theta_e. \tag{13}$$

Here, the gain matrices K_r, K_v, and K_θ are the blocks of K associated with the states r, v, and θ, respectively.

By incorporating an additional term into the linear control law (13), it is modified for the purpose of trajectory tracking. Suppose that $r_d(t) \in \mathscr{C}$ is a trajectory near the point $r = 0$, and the magnetic bead must be steered along this trajectory. This task is performed by a state feedback law of the form

$$u(t) = -K_r r(t) - K_v v(t) - K_\theta(\theta(t) - \theta_e) + \theta_e + K_d r_d(t), \tag{14}$$

where the gain matrix K_d is given by

$$K_d = -\left(C (A - BK)^{-1} B \right)^\dagger.$$

Here, $\dagger$ denotes the Moore-Penrose inverse of matrices.

C. Performance Optimization

As indicated by (9), the matrix A in the approximate linear model (8) depends on the actual value of θ_e, which creates an equilibrium point by solving the algebraic equation (7). Thus, the solution $P = P(\theta_e)$ to the Riccati equation (12), and as a result, the gain matrices K_r, K_v, K_θ, and K_d in the control law (14) are functions of θ_e. Hence, the performance of this control law must depend on the specific value of θ_e, and can be optimized by obtaining an optimal value of $\theta_e = \theta_e^*$.

The optimality measure to obtain the best value of $\theta_e = \theta_e^*$ can be derived from the cost function (10). It is well-known that under the optimal control (11), this cost function attains its minimum value [31]

$$J^*(\theta_e) = x_e^T(0) P(\theta_e) x_e(0). \tag{15}$$

Then, it is reasonable to minimize this function with respect to θ_e in order to obtain the optimal value $\theta_e = \theta_e^*$. Of course, the value of $x_e(0)$ on the right-hand side of (15) is not known in advance, so the maximum value

$$\|P(\theta_e)\| = \max_{\|x_e(0)\|=1} x_e^T(0) P(\theta_e) x_e(0)$$

of the right-hand side can be alternatively minimized. Noting that θ_e must solve the algebraic equation (7), the best value of $\theta_e = \theta_e^*$ is given by the constrained optimization problem

$$\begin{aligned} \min_{\theta_e \in [0, 2\pi]^n} \quad & \|P(\theta_e)\| \\ \text{s.t.} \quad & g(0, \theta_e) = 0. \end{aligned} \tag{16}$$

The solution to this optimization problem is a vector with generally unequal elements. Such asymmetric structure of θ_e results in an anisotropic control that performs differently in different directions along which a magnetic object is driven. Particularly, the operation subregion over which the magnetic object can be effectively steered will not preserve the same symmetry of the magnetic manipulator. To keep the control isotropic, an additional constraint on θ_e is imposed to ensure its elements are equal, i.e., $\theta_e = \vartheta \mathrm{i}$, where ϑ is a scalar and i is an $n \times 1$ vector of unit elements. With this constraint on θ_e, the geometric symmetry of the magnetic manipulator implies that $g(0, \vartheta \mathrm{i}) = 0$ identically holds for every ϑ. Therefore, the constrained optimization problem (16) is reduced into the unconstrained scalar problem

$$\min_{\vartheta \in [0, \pi/2]} \quad \|P(\vartheta \mathrm{i})\|. \tag{17}$$

Because of the geometric symmetry, this optimization is only performed over $\vartheta \in [0, \pi/2]$ rather than $[0, 2\pi]$.

IV. Numerical Simulation

We developed computer simulations to study the magnetic manipulator of Fig. 1 under feedback control. Our simulator numerically solves the nonlinear state-space equations (6) for control inputs generated by the linear feedback law (14). The simulation results were generated for a setup with $n = 6$ disc magnets of radius $b = 0.5$ and thickness $d = 0.1$, arranged around a circular container of radius $a = 1$. The values taken for other parameters are $k_g = 1$, $\sigma_v = 1$, and $\sigma_s = 10$. The magnetic field $h_c(\cdot)$ of the disc magnets was calculated from an analytical formula existing in the literature [35]. To ensure the credibility of our simulations, we evaluated the accuracy of this formula experimentally [36].

The gain matrices K_r, K_v, and K_θ were determined using the `care` function of MATLAB with $Q = \mathrm{diag}(I_2, I_2, 0_n)$ and $R = I_n$. The optimal value of ϑ is obtained as $\vartheta^* = 9^\circ$ by solving the optimization problem (17), as shown in Fig. 4. According to this figure, the control performance drastically improves at the optimal value $\vartheta^* = 9^\circ$ as compared to more trivial values at $\vartheta = 0$ or $\vartheta = \pi/2$.

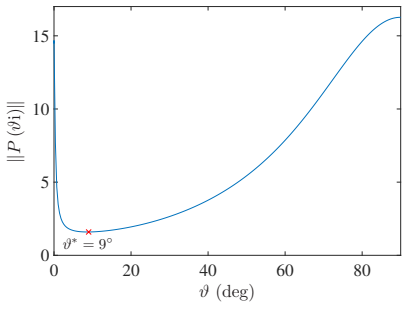

Fig. 4. Performance optimization by solving the optimization problem (17). The values of $\|P(\vartheta \mathrm{i})\|$ are illustrated versus ϑ and the minimum is attained at the minimizer $\vartheta^* = 9^\circ$.

A key simulation result indicates that the control law (14) can stabilize the unstable equilibrium at $x = 0$. For different initial states, the state trajectories of the closed-loop system were constructed under $r_d(t) = 0$ to examine whether they approach the equilibrium at $x = 0$. By generating a large number of such state trajectories with different initial states, the region of attraction (ROA) was numerically constructed for this equilibrium.

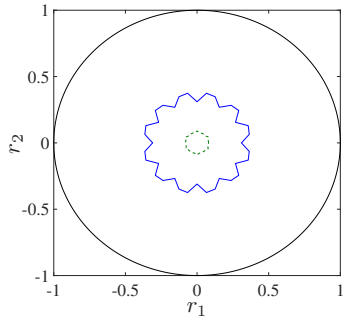

Fig. 5. Cross section of ROA with the hyperplane $(v, \theta) = (0, \theta_e)$ under the state feedback (14), with the optimal value $\vartheta = \vartheta^* = 9^\circ$ (solid line), and with the trivial value $\vartheta = 0$ (dashed line).

The ROA associated with the equilibrium $x = 0$ is the set of all initial states for which the state trajectory tends toward $x = 0$ under $r_d(t) = 0$. The size of this set is a key measure for the stability of a system, and a major performance index for a feedback controller. The cross section of ROA with the hyperplane $(v, \theta) = (0, \theta_e)$ is shown in Fig. 5 for an optimal controller with $\vartheta = \vartheta^* = 9^\circ$ and for a baseline controller with $\vartheta = 0$. This figure indicates that both linear controllers are indeed able to stabilize a magnetic manipulator of highly nonlinear nature, but only over some subregion of its entire operation region (the circular region in Fig. 5). Moreover, optimizing the feedback law with respect to the linearization point θ_e substantially enlarges this subregion.

The performance of trajectory tracking is investigated next. A complex SIU-shaped path inside ROA is considered as the reference trajectory $r_d(t)$. The trajectory of a magnetic bead driven along this reference trajectory is illustrated in Fig. 6. It is observed in Fig. 6(a) that for a reference trajectory within a 0.4×0.4 box around the center, the actual trajectory of the magnetic bead stays rather close to the reference trajectory, which indicates the effectiveness of the proposed control law. As the extent of the reference trajectory grows in Fig. 6(b) beyond the box, the tracking error becomes more significant, due to the approximate model utilized for control design. If the reference trajectory grows further beyond Fig. 6(b), the feedback loop fails and the close-loop system turns unstable.

V. Conclusion

The performance of a permanent magnet manipulator was studied under linear feedback control. This manipulator uses an array of permanent magnets to precisely drive a magnetic object along an arbitrary reference trajectory without direct contact. The magnets are equipped with servomotors in order to control their directions, and as a result, the total magnetic force they apply to the magnetic object. It was shown that the dynamics of this object under the magnetic force is nonlinear and unstable, but it can be stabilized by means of feedback

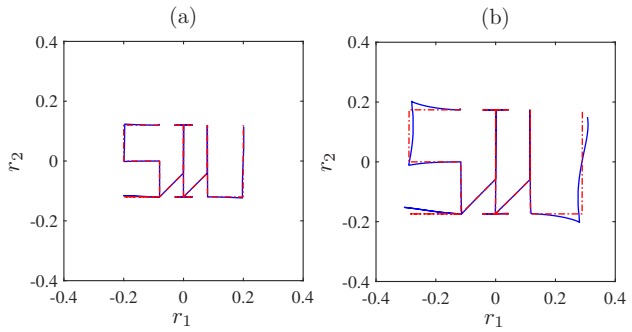

Fig. 6. Trajectories of a magnetic bead (solid line) tracking a SIU-shaped reference trajectory (dashed line) under the state feedback (14). As the size of the reference trajectory increases from (a) to (b), the tracking error becomes more significant.

control. A linear state feedback was developed via the LQR method and was optimized for the most effective stabilization and tracking performance. The main advantages of this linear control law over its high performance nonlinear counterparts are its low computational complexity, and the possibility for easy tuning of its parameters.

REFERENCES

[1] N. Riahi and A. Komaee, "Steering magnetic particles by feedback control of permanent magnet manipulators," in *Proc. of 2019 American Control Conference (ACC 2019)*, pp. 5432–5437, 2019.

[2] N. Riahi, L. R. Tituaña, and A. Komaee, "Homotopy continuation for feedback linearization of noncontact magnetic manipulators," in *Proc. of 2020 American Control Conference (ACC 2020)*, will appear 2020.

[3] F. M. Creighton, *Control of magnetomotive actuators for an implanted object in brain and phantom materials*. PhD thesis, University of Virginia, 1991.

[4] E. G. Quate, K. G. Wika, M. A. Lawson, G. T. Gillies, R. C. Ritter, M. S. Grady, and M. A. Howard, "Goniometric motion controller for the superconducting coil in a magnetic Stereotaxis system," *IEEE Trans. Biomed. Eng.*, vol. 38, no. 9, pp. 899–905, 1991.

[5] A. Komaee and B. Shapiro, "Steering a ferromagnetic particle by magnetic feedback control: Algorithm design and validation," in *Proc. of 2010 American Control Conference (ACC 2010)*, pp. 6543–6548, 2010.

[6] M. P. Kummer, J. J. Abbott, B. E. Kratochvil, R. Borer, A. Sengul, and B. J. Nelson, "OctoMag: An electromagnetic system for 5-DOF wireless micromanipulation," *IEEE Trans. Robot.*, vol. 26, no. 6, pp. 1006–1017, 2010.

[7] R. Probst, J. Lin, A. Komaee, A. Nacev, Z. Cummins, and B. Shapiro, "Planar steering of a single ferrofluid drop by optimal minimum power dynamic feedback control of four electromagnets at a distance," *J MAGN MAGN MATER*, vol. 323, no. 7, pp. 885–896, 2011.

[8] A. Komaee and B. Shapiro, "Steering a ferromagnetic particle by optimal magnetic feedback control," *IEEE Trans. Control Syst. Technol.*, vol. 20, no. 4, pp. 1011–1024, 2012.

[9] S. Afshar, M. B. Khamesee, and A. Khajepour, "Optimal configuration for electromagnets and coils in magnetic actuators," *IEEE Trans. Magn.*, vol. 49, no. 4, pp. 1372–1381, 2013.

[10] O. Baun and P. Blümler, "Permanent magnet system to guide superparamagnetic particles," *J MAGN MAGN MATER*, vol. 439, pp. 294–304, 2017.

[11] M. Sendoh, K. Ishiyama, and K.-I. Arai, "Fabrication of magnetic actuator for use in a capsule endoscope," *IEEE Trans. Magn.*, vol. 39, no. 5, pp. 3232–3234, 2003.

[12] G. Ciuti, P. Valdastri, A. Menciassi, and P. Dario, "Robotic magnetic steering and locomotion of capsule endoscope for diagnostic and surgical endoluminal procedures," *Robotica*, vol. 28, no. 2, pp. 199–207, 2010.

[13] M. Simi, P. Valdastri, C. Quaglia, A. Menciassi, and P. Dario, "Design, fabrication, and testing of a capsule with hybrid locomotion for gastrointestinal tract exploration," *IEEE/ASME Trans. Mechatronics*, vol. 15, no. 2, pp. 170–180, 2010.

[14] A. Komaee and B. Shapiro, "Magnetic steering of a distributed ferrofluid spot towards a deep target with minimal spreading," in *Proc. of 50th IEEE Conference on Decision and Control and European Control Conference*, pp. 7950–7955, Dec. 2011.

[15] S. Yim and M. Sitti, "Design and rolling locomotion of a magnetically actuated soft capsule endoscope," *IEEE Trans. Robot.*, vol. 28, no. 1, pp. 183–194, 2012.

[16] A. Nacev, A. Komaee, A. Sarwar, R. Probst, S. H. Kim, M. Emmert-Buck, and B. Shapiro, "Towards control of magnetic fluids in patients: directing therapeutic nanoparticles to disease locations," *IEEE Control Syst. Mag.*, vol. 32, no. 3, pp. 32–74, 2012.

[17] A. Komaee, R. Lee, A. Nacev, R. Probst, A. Sarwar, D. A. Depireux, K. J. Dormer, I. Rutel, and B. Shapiro, *Magnetic Nanoparticles: From Fabrication to Clinical Applications*, ch. Putting Therapeutic Nanoparticles Where They Need to Go by Magnet Systems Design and Control, pp. 419–448. CRC Press, 2012.

[18] M. Beccani, C. Di Natali, L. J. Sliker, J. A. Schoen, M. E. Rentschler, and P. Valdastri, "Wireless tissue palpation for intraoperative detection of lumps in the soft tissue," *IEEE Trans. Biomed. Eng.*, vol. 61, no. 2, pp. 353–361, 2014.

[19] V. Iacovacci, L. Ricotti, P. Dario, and A. Menciassi, "Design and development of a mechatronic system for noninvasive refilling of implantable artificial pancreas," *IEEE/ASME Trans. Mechatronics*, vol. 20, no. 3, pp. 1160–1169, 2015.

[20] L. Sliker, G. Ciuti, M. Rentschler, and A. Menciassi, "Magnetically driven medical devices: a review," *Expert Review of Medical Devices*, vol. 12, no. 6, pp. 737–752, 2015.

[21] A. Komaee, "Feedback control for transportation of magnetic fluids with minimal dispersion: A first step toward targeted magnetic drug delivery," *IEEE Trans. Control Syst. Technol.*, vol. 25, no. 1, pp. 129–144, 2017.

[22] C. Gosse and V. Croquette, "Magnetic tweezers: Micromanipulation and force measurement at the molecular level," *Biophysical Journal*, vol. 82, no. 6, pp. 3314–3329, 2002.

[23] M. B. Khamesee, N. Kato, Y. Nomura, and T. Nakamura, "Design and control of a microrobotic system using magnetic levitation," *IEEE/ASME Trans. Mechatronics*, vol. 7, no. 1, pp. 1–14, 2002.

[24] N. Pamme, "Magnetism and microfluidics," *Lab on a Chip*, vol. 6, no. 1, pp. 24–38, 2006.

[25] M. A. M. Gijs, F. Lacharme, and U. Lehmann, "Microfluidic applications of magnetic particles for biological analysis and catalysis," *Chemical Reviews*, vol. 110, no. 3, pp. 1518–1563, 2009.

[26] S. Schuerle, S. Erni, M. Flink, B. E. Kratochvil, and B. J. Nelson, "Three-dimensional magnetic manipulation of micro- and nanostructures for applications in life sciences," *IEEE Trans. Magn.*, vol. 49, no. 1, pp. 321–330, 2013.

[27] H. Marino, C. Bergeles, and B. J. Nelson, "Robust electromagnetic control of microrobots under force and localization uncertainties," *IEEE Trans. Autom. Sci. Eng.*, vol. 11, no. 1, pp. 310–316, 2014.

[28] D. G. Latcu, P. Ricard, N. Zarqane, K. Yaici, J.-P. Rinaldi, A. Maluski, and N. Saoudi, "Robotic magnetic navigation for ablation of human arrhythmias: Initial experience," *Archives of Cardiovascular Diseases*, vol. 102, no. 5, pp. 419–425, 2009.

[29] S. Earnshaw, "On the nature of the molecular forces which regulate the constitution of the luminferous ether," *Transactions of the Cambridge Philosophical Society*, vol. 7, pp. 97–112, 1842.

[30] H. K. Khalil, *Nonlinear Systems*. Upper Saddle River: Prentice-Hall, Inc., 2002.

[31] J. P. Hespanha, *Linear Systems Theory*. Princeton, NJ: Princeton University Press, 2009.

[32] Q. A. Pankhurst, J. Connolly, S. K. Jones, and J. Dobson, "Applications of magnetic nanoparticles in biomedicine," *Journal of physics D: Applied physics*, vol. 36, no. 13, p. R167, 2003.

[33] C. I. Mikkelsen, *Magnetic separation and hydrodynamic interactions in microfluidic systems*. PhD thesis, Technical University of Denmark, 2005.

[34] R. F. Probstein, *Physicochemical Hydrodynamics: An Introduction*. New York: Wiley, 1994.

[35] M. Fontana, F. Salsedo, and M. Bergamasco, "Novel magnetic sensing approach with improved linearity," *Sensors*, vol. 13, no. 6, pp. 7618–7632, 2013.

[36] N. Riahi and A. Komaee, "Experimental validation of an analytical model for diametrically magnetized permanent magnets," in *Proc. of Annual Conference on Magnetism and Magnetic Materials*, (Las Vegas, NV), 2019.